ISBN: 978-3-95450-184-7 doi:10.18429/JACoW-IPAC2018-THPAK065

APPLICATION OF TRANSVERSE-TO-LONGITUDINAL PHASE-SPACE-EXCHANGED BEAM PRODUCED FROM A NANO-STRUCTURE PHOTOCATHODE TO A SOFT X-RAY FREE-ELECTRON LASER

A. Lueangaramwong*, P. Piot[1]
Department of Physics and Northern Illinois Center for Accelerator & Detector Development, Northern Illinois University, DeKalb, IL 60115, USA
G. Andonian, RadiaBeam, Santa Monica, CA 90404, USA
[1]also at Fermi National Accelerator Laboratory, Batavia, IL 60510, USA

Abstract

Nano-structured cathodes can form transversely modulated beams which can be subsequently converted to temporally modulated beam via a transverse-to-longitudinal phase space-exchanging beamline. We demonstrate via numerical simulation the generation of transversely modulated beam at the nm scale and investigate the corresponding enhancement in a soft-X-ray SASE free-electron laser. Our study is supported by start-to-end simulation combining WARP, IMPACT-T and GENESIS (FEL process) and focuses on the optimization of the beamline to preserve initial modulation at the nanometer level. We also discuss the scaling of the concept to shorter-wavelengths.

INTRODUCTION

Temporally modulated beam has become one of important keys to modern soft-X-ray SASE free-electron lasers. We have developed an alternative method of the required temporally modulated beam using a transverse-to-longitudinal phase space-exchanging beamline. Thus, this method employs transversely modulated beams which can be produced by plasmonic photocathodes.

Plasmonic photocathodes have recently demonstrated enhanced quantum efficiency, owing to both higher laser field absorption and field enhancement at sharp edges of each nano-structure. The cathode employs a surface engineered at the nanometer scale with periodicity matching with the excitation laser wavelength. For instance, the periodic structure can be a two-dimensional pattern or array of tips or holes [1, 2], or a series of tranches organized as a grating.

Since each nano-structure generates a beamlet, the nanoscale pattern dictates the beam initial distribution and could form density-modulated beams. Such transversely-modulated beams has been numerically investigated. We showed that information related to the initial patterned distribution (on the cathode surface) for the subsequent imaging after acceleration to relativistic energies could be preserved [3]. The simulations of the beam dynamics, is performed piecewise by combining the WARP [4] simulation framework with the IMPACT-T [5] beam dynamics program. WARP is employed to investigate the beam dynamic in the vicinity of the cathode while IMPACT-T tracked the emitted electrons through an RF-gun and a linear acceleration (Linac) for acceleration to relativistic energies.

The beam distributions simulated with IMPACT-T downstream from the acceleration are used as an input into ELEGANT. A set of quadupole magnets can be implemented for the transverse-matching conditions derived in Ref. [6]. We successfully simplified the task by using a single quadrupole magnet and tuning its strength to provide an image of transversely-modulated beams in the (x, x') phase space shown in [3].

The transversely-modulated beams could be directly applied to a variety of applications or further manipulated, e.g., using transverse-to-longitudinal phase-space exchangers to yield temporally-modulated electron bunches [7, 8].

In this paper, we show that we can adapt the matching conditions to provide an image of temporally-modulated beam when combining a single quadrupole magnet emittance exchanger (EEX) after the acceleration to relativistic energies (as illustrated in Fig. 1).

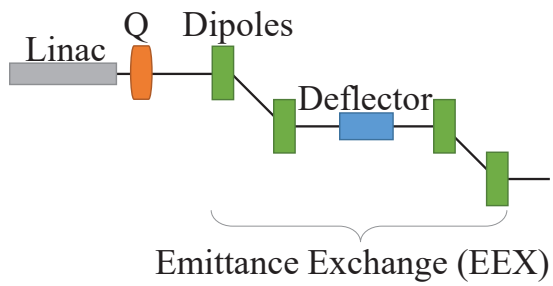

Figure 1: Schematic of EEX line combined with a quadrupole magnet (Q) tuned for the matching conditions, which locates at downstream end of Linac.

TRANSVERSELY-MODULATED BEAMS IN ACCELERATION TO RELATIVISTIC ENERGIES

The simulations uses an idealized distribution with parameters consistent with the distribution simulation with WARP shown in [6]. We study transversely-modulated beams described as 3×3 array with nano-structure periodicity of 1.6 microns.

* anusorn@nicadd.niu.edu

ISBN: 978-3-95450-184-7 doi:10.18429/JACoW-IPAC2018-THPAK065

The cathode is located on the back plate of a standard $1+\frac{1}{2}$-cell RF gun of BNL/SLAC/UCLA type operating at the S-band frequency and a following 3-cell S-band traveling-wave accelerating section thereby boosting the beam energy to 47.2 MeV. See RF-gun and photocathode-laser parameters in [3]. The traveling wave structure employs the supperposition of two standing wave strutures [9].

The dynamics was simulated in IMPACT-T employing a point-to-point N-body space charge solver. After the accelerations, beamlets in the transversely-modulated beam are no more transversely separated due to the large correlated divergence they acquired. However the information is preserved in the phase space where the beamlets keep apart; see Fig. 2 and [3] for only acceleration by an RF gun.

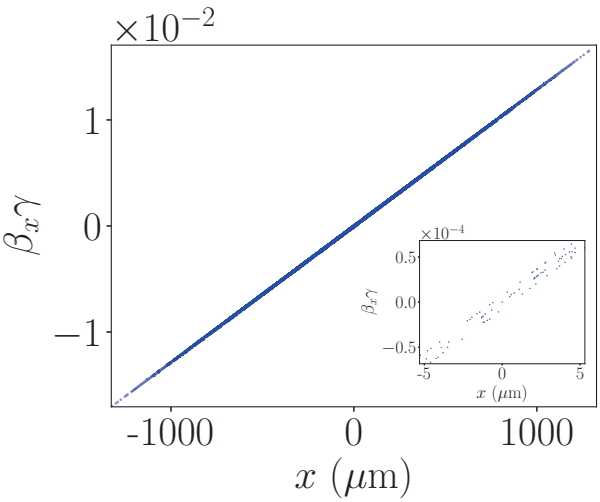

Figure 2: Transverse phase space associated to the 3×3-hole array emitter downstream of the Linac at z = 3.693 m from the cathode surface.

MATCHING CONDITIONS FOR TRANSVERSE-TO-LONGITUDINAL PHASE-SPACE-EXCHANGING

At downstream end of the accelerations, the Courant-Snyder parameters [for the horizontal plane $(\alpha_{x,1}, \beta_{x,1})$] associated to a single beamlet (formed by a nano-structure) along with the parameters computed of the entire beam (α_x, β_x) are considered for matching conditions represented by a transformation matrix **R**. Given transformation matrix elements R_{ij}, the transverse-matching condition $R_{12}/R_{11} = \beta_{x,1}/\alpha_{x,1}$ retrieves modulation along x-axis (beamlet separation; see Fig. 4 in [3]), while $R_{22}/R_{21} = \beta_{x,1}/\alpha_{x,1}$ gives modulation along x'-axis (separation of beamlet momenta in x-direction); see derivation in [10].

Similarly, $R_{52}/R_{51} = \beta_{x,1}/\alpha_{x,1}$ can provide temporal modulation. However, EEX alone does not have flexibility to achieve this matching condition. A single quadrupole magnet may be inserted in front of an EEX to make R_{51} and R_{52} adjustable.

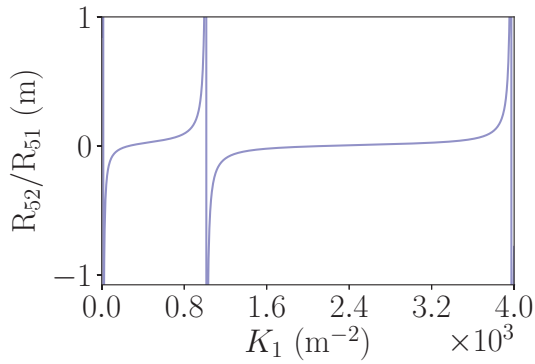

Figure 3: Plot of R_{52}/R_{51} as a function of a single quadrupole magnet parameter K_1 with L_Q = 10 cm and L_d of 50 cm for a focusing quadrupole magnet and a following drift. A sample ideal EEX with R_{51} = -0.176, R_{52} = -0.043, R_{61} = -5.27 and R_{62} = -6.97 is applied.

The plot in Fig. 3 shows that K_1 in range of (12.8, 272.5) m^{-2} gives the negative R_{52}/R_{51} (as now beam is defocusing after acceleration) as well as minimum defocusing force in vertical direction y. This range of K_1 is used in ELEGANT to optimize parameters of focusing quadrupole magnets in a beam line. Moreover, one can also simply prove that longer drift length L_d decreases the K_1 range.

IMAGING AT EEX

The matching conditions were studied by using ELEGANT. ELEGANT can solve matching conditions and track particle trajectories including acceleration to 1.5 GeV, while importing beam distribution to start with.

The beam distribution simulated with IMPACT-T at z = 3.693 m downstream from the cathode surface shown in Fig. 2 has $\beta_{x,1}/\alpha_{x,1}$ of -7.1538 m with corresponding K_1 of 14.307 m^{-2}. However, we manually choose K_1 of 14.338 m^{-2} instead to obtain the temporal modulation.

The plots in Fig 4 shows a temporal modulation in the longitudinal phase space. Thus we estimated a bunching factor from the modulation for study of FELs power.

SIMULATION OF FEL POWER

In this study, We use the calculated bunching factor and undulator parameters shown in Table 1 for simulations in GENESIS program.

Fig. 5 shows a promising plot of FELs radiation power as a function of longitudinal distance that beam traveling in the undulator. Our first start-to-end simulation combining WARP, IMPACT-T and GENESIS has shown possibilities of employing beam from nano-structured (plasmonic) cathode in producing a soft x-ray free electron laser.

ISBN: 978-3-95450-184-7 doi:10.18429/JACoW-IPAC2018-THPAK065

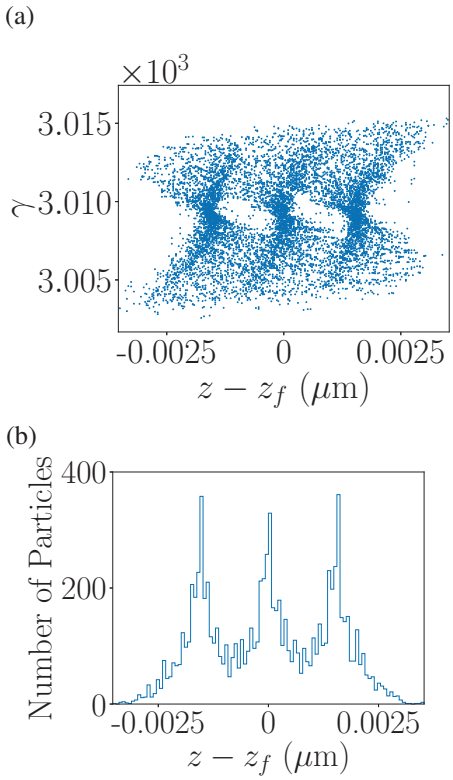

Figure 4: Longitudinal phase space (a) and its projections (b) at EEX exit $z = z_f$ m after a single quadrupole magnet tuned to temporal modulation.

Table 1: Beam and Undulator Parameters Used for FELs Simulations in GENESIS Program

Parameter	Symbol	Nominal	Unit
radiation wavelength	λ	1.555	nm
normalized rms undulator parameter	a_u	0.93	–
undulator period length	λ_u	1.5	cm
beam energy	E	1.5	GeV
bunching factor	B_f	7.22×10^{-2}	–
beam peak current	I_p	122.4	A
normalized emittance in x	$\epsilon_{n,x}$	1.93×10^{-7}	m
normalized emittance in y	$\epsilon_{n,y}$	3.69×10^{-9}	m
beam size in x	σ_x	2×10^{-4}	m
beam size in y	σ_y	6×10^{-4}	m

FUTURE PLANS

We plan to study and correct temporal aberration in EEX for this application. Beam from larger sizes of nanohole array will be studied to confirm our concept.

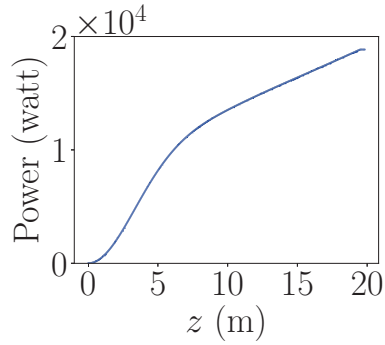

Figure 5: Plot of FELs radiation power as a function of longitudinal distance that beam traveling in the undulator.

ACKNOWLEDGEMENTS

This work was supported by the US Department of Energy (DOE) under contract DE-SC0009656 with Radiabeam Technologies and by the National Science Foundation under Grant PHY-1535401 with Northern Illinois University.

REFERENCES

[1] R. K. Li, H. To, G. Andonian, J. Feng, A. Polyakov, C. M. Scoby, K. Thompson, W. Wan, H. A. Padmore, and P. Musumeci, *Phys. Rev. Lett.*, vol. 110, p. 074801, 2013.

[2] A. Polyakov, C. Senft, K. F. Thompson, J. Feng, S. Cabrini, P. J. Schuck, H. A. Padmore, S. J. Peppernick, and W. P. Hess, *Phys. Rev. Lett.*, vol. 110, p. 076802, 2013.

[3] A. Lueangaramwong, D. Mihalcea, G. Andonian and P. Piot, in *Proc. IPAC'17*, Copenhagen, Denmark, May 2017, pp.545-547.

[4] J.-L. Vay, D. P. Grote, R. H. Cohen and A. Friedman, *Computational Science & Discovery*, vol. 5, p. 014019, 2012.

[5] J. Qiang, S. Lidia, R. D. Ryne, and C. Limborg-Deprey, *Phys. Rev. ST Accel. Beams*, vol. 9, p. 044204, 2006 ; J. Qiang, R. Ryne, S. Habib, and V. Decyk, *J. Comp. Phys.*, vol. 163, p. 434, 2000.

[6] A. Lueangaramwong, D. Mihalcea, G. Andonian and P. Piot, *Nucl. Instrum. Meth. Sec. A*, vol. 865, pp. 119-124, 2017.

[7] Y.-E Sun, P. Piot, A. Johnson, A. H. Lumpkin, T. J. Maxwell, J. Ruan, and R. Thurman-Keup, *Phys. Rev. Lett.*, vol. 105, p. 234801, 2010.

[8] W. S. Graves, F. X. Kärtner, D. E. Moncton, and P. Piot, *Phys. Rev. Lett.*, vol. 108, p. 263904, 2012.

[9] G. A. Lowe, R. H. Miller, R. A. Early and K. L. Bane, *IEEE Trans. Nucl. Sci.*, vol. 26, no. 3, p. 3701, 1979.

[10] A. Lueangaramwong, G. Andonian and P. Piot, in preparation, 2018.